



**HAL**  
open science

## The local environment orchestrates mucosal decidual macrophage differentiation and substantially inhibits HIV-1 replication.

E El Costa, F Quillay, E Marlin, F Cannou, E Duriez, F Benjelloun, Claire de Truchis, F Rahmati, F Ighil, Françoise Barré-Sinoussi, et al.

### ► To cite this version:

E El Costa, F Quillay, E Marlin, F Cannou, E Duriez, et al.. The local environment orchestrates mucosal decidual macrophage differentiation and substantially inhibits HIV-1 replication.. *Mucosal Immunology*, 2016, 9 (3), pp.634-46. 10.1038/mi.2015.87 . pasteur-01453433

**HAL Id: pasteur-01453433**

**<https://pasteur.hal.science/pasteur-01453433>**

Submitted on 13 Feb 2017

**HAL** is a multi-disciplinary open access archive for the deposit and dissemination of scientific research documents, whether they are published or not. The documents may come from teaching and research institutions in France or abroad, or from public or private research centers.

L'archive ouverte pluridisciplinaire **HAL**, est destinée au dépôt et à la diffusion de documents scientifiques de niveau recherche, publiés ou non, émanant des établissements d'enseignement et de recherche français ou étrangers, des laboratoires publics ou privés.



Distributed under a Creative Commons Attribution - NonCommercial - NoDerivatives 4.0 International License

1 **The local environment orchestrates mucosal decidual macrophage**  
2 **differentiation and substantially inhibits HIV-1 replication**

3

4 H El Costa<sup>1</sup>, H Quillay<sup>1,2</sup>, R Marlin<sup>3,4,5,6</sup>, C Cannou<sup>1</sup>, M Duriez<sup>7</sup>, F Benjelloun<sup>1</sup>, C de  
5 Truchis<sup>8</sup>, M Rahmati<sup>9</sup>, J Ighil<sup>9</sup>, F Barré-Sinoussi<sup>1</sup>, M T Nugeyre<sup>1</sup>, E Menu<sup>1,3,4,5,\*</sup>

6

7 <sup>1</sup>Institut Pasteur, Regulation of Retroviral Infection Unit, Paris, France

8 <sup>2</sup>Université Paris Diderot, Sorbonne Paris Cité, Cellule Pasteur, Paris, France

9 <sup>3</sup>Université Paris Sud, UMR 1184, France

10 <sup>4</sup>CEA, DSV/iMETI, Division of Immuno-Virology, IDMIT, France

11 <sup>5</sup>Inserm, U1184, Center for immunology of viral infections and autoimmune diseases,  
12 France

13 <sup>6</sup>Vaccine Research Institute (VRI), Créteil, France

14 <sup>7</sup>Sorbonne Universités, UPMC Univ Paris 06, INSERM U1135, Centre d'Immunologie  
15 et des Maladies Infectieuses (CIMI), Persistent Viral Infections (PVI) Team, Paris,  
16 France

17 <sup>8</sup>Gynecology-Obstetrics Service, A. Béclère Hospital, AP-HP, Clamart, France

18 <sup>9</sup>Gynecology-Obstetrics Service, Pitié Salpêtrière Hospital AP-HP, Paris, France.

19

20 \* Correspondence : E Menu, [elisabeth.menu@pasteur.fr](mailto:elisabeth.menu@pasteur.fr)

21 **Abstract**

22

23 Macrophages from the *decidua basalis* (dM), the main uterine mucosa during  
24 pregnancy, are weakly permissive to HIV-1 infection. Here we investigated the  
25 mechanisms underlying this natural control. We show, by using freshly purified  
26 decidual macrophages and *ex vivo* human decidual explants, that the local decidual  
27 environment influences dM differentiation and naturally protects these cells from HIV-  
28 1 infection. IFN- $\gamma$ , present in the decidual tissue, contributes to maintenance of the  
29 dM phenotype and restricts HIV-1 infection by mechanisms involving the cyclin-  
30 dependent kinase inhibitor p21Cip1/Waf1. We also found that activation of Toll-like  
31 receptors 7 and 8 expressed by dM reinforces the low permissivity of dM to HIV-1 by  
32 restricting viral replication and inducing secretion of cytokines in the decidual  
33 environment, including IFN- $\gamma$ , that shape dM plasticity. A major challenge for HIV-1  
34 eradication is to control infection of tissue-resident macrophages in the female  
35 reproductive tract. Our findings provide clues to the development of novel strategies  
36 to prevent HIV-1 macrophage infection.

## 37 **Introduction**

38

39 The *decidua basalis*, the main uterine mucosa during pregnancy, is a model for  
40 studying natural protection against HIV-1 mucosal infection. Indeed, maternofetal  
41 HIV-1 transmission is rare during the first trimester, and HIV-1 dissemination appears  
42 to be tightly controlled at the maternofetal interface <sup>1</sup>. Macrophages that reside in  
43 decidual tissue (dM) are fully differentiated. They are the main targets of CCR5-tropic  
44 HIV-1 but are less permissive to HIV-1 infection than their peripheral blood  
45 counterparts <sup>2</sup>.

46 The *decidua basalis* is characterized by a specific pro/anti-inflammatory cytokine  
47 balance required to support fetal development. These cytokines maintain a state of  
48 local immune tolerance to the semi-allogeneic fetus and probably ensure host  
49 defenses against pathogens <sup>3</sup>.

50 Pro- and anti-inflammatory cytokines trigger peripheral monocyte derived  
51 macrophage (MDM) differentiation into opposing programs. This polarization gives  
52 rise to two major macrophage phenotypes, designated M1 (classic) and M2  
53 (alternative). M1 macrophages generated in response to cytokines such as IFN- $\gamma$  and  
54 TNF- $\alpha$ , produce pro-inflammatory cytokines such as IL-12 and TNF- $\alpha$  and mediate  
55 resistance to pathogens. They express the transcription factor IRF5<sup>4</sup>, the  
56 costimulatory molecules CD80 and CD86, and the FC $\gamma$  receptor I CD64 <sup>5,6</sup>. M2  
57 macrophages, generated in response to cytokines such as IL-10, produce anti-  
58 inflammatory cytokines (especially IL-10 and IL1-RA) and promote tissue remodeling.  
59 The surface-marker expression profile of M2 macrophages includes the scavenger  
60 receptor CD163 and the mannose receptor CD206 <sup>5,6</sup>. This MDM plasticity is linked  
61 to HIV-1 susceptibility <sup>7</sup>.

62 Decidual macrophages have an M2-like phenotype and show features of pro-  
63 inflammatory and tolerogenic macrophages, simultaneously expressing M1 (CD64,  
64 CD80, CD86) and M2 markers (CD163, CD206)<sup>2,8</sup>.

65 Another hallmark of the *decidua basalis* is the abundance of decidual natural killer  
66 cells (dNK). The dNK cells secrete large amounts of IFN- $\gamma$  and TNF- $\alpha$  and are  
67 involved in the control of fetal cell invasion, initiation of endometrial vasculature.  
68 These cells may limit also the spreading of viral infection to fetal tissues by  
69 controlling intrauterine infection by hCMV<sup>9</sup> and HIV-1 (Quillay et al., manuscript  
70 under revision).

71 dM and dNK cells express innate receptors, such as toll-like receptors 7 and 8  
72 (TLR7/8), that sense HIV-1 sequences and are involved in mediating immune  
73 activation following HIV-1 infection<sup>3,10</sup>. We have shown that, upon TLR7/8 activation,  
74 dM and dNK cells secrete large amounts of cytokines<sup>3</sup>. TLR7/8 activation inhibits  
75 HIV-1 replication in monocytes and MDM<sup>11-14</sup>. In addition, TLR7/8 may influence  
76 macrophage polarization, either by activating signaling pathways or by inducing the  
77 secretion of cytokines associated with macrophage polarization in the  
78 microenvironment<sup>3,14-16</sup>.

79 The aim of this work was to determine why dM are weakly permissive to HIV-1  
80 infection during the first trimester of pregnancy, with a view to the development of  
81 novel strategies for eradicating macrophage infection. We postulated that the  
82 decidual environment must contain factors that shape dM plasticity and susceptibility  
83 to HIV-1 infection, and that TLR7/8, if activated, can reinforce this low dM  
84 permissivity by modulating the local environment and blocking HIV-1 replication.

## 85 **Results**

86

### 87 **dM in culture undergo dynamic changes toward a more M2 profile and become** 88 **more permissive to HIV-1 infection**

89 To address whether the local decidual environment influences the susceptibility of  
90 dM to HIV-1 infection, dM were isolated and challenged with VSV-G pseudotyped  
91 HIV-1 (HIV-1/VSV-G), immediately after purification (day 0) or after 3 or 7 days of  
92 culture in cytokine-free medium. HIV-1 replication was monitored by measuring  
93 luciferase activity. Surprisingly, we found that freshly purified dM had very low  
94 permissivity to HIV-1/VSV-G but became more susceptible with time in culture  
95 (Figure 1a). Similar results were obtained when freshly purified dM and cultured dM  
96 were challenged with CCR5-using macrophage-tropic HIV-1<sub>BaL</sub>, as shown by p24 Ag  
97 measurement (Figure 1b).

98 To explain these results, we monitored the surface expression of several  
99 macrophage markers by flow cytometry. Expression of M2 markers (CD163, CD206)  
100 increased in culture (Figures 2a and 2b), whereas expression of M1 markers (CD64,  
101 CD80, CD86) remained unchanged (Supplementary figure S1). We then analyzed  
102 HIV-1 receptor and co-receptor expression (CD4, CCR5 and DC-SIGN) and found  
103 that only CCR5 expression increased significantly over time (Figure 2c). Early after  
104 purification, these cells consisted of approximately equal numbers of spindle-shaped  
105 fibroblastoid cells and large flat-round cells (Supplementary figure S2a, left panel),  
106 whereas round-shaped cells gradually became predominant in culture  
107 (Supplementary figure S2a, right panel). This suggested that dM polarization  
108 switched towards a more M2 profile in culture. To confirm this, we used western blot  
109 to analyze the expression of the M1 transcription factor (IRF5) involved in the M2 to  
110 M1 switch. In keeping with our previous observations, IRF5 expression was

111 decreased gradually in culture (Figure 2d). Analysis of cytokine secretion showed  
112 that dM maintained their secretion of M2 cytokines (IL-1RA and IL-10) over time  
113 (Figure 2e).

114 Together, these results indicate that dM isolated from their local environment  
115 acquire more M2 features and that this switch is accompanied by an increase in  
116 susceptibility to HIV-1 infection.

117

### 118 **IFN- $\gamma$ participates in dM differentiation and in resistance to HIV-1 infection**

119 The next step was to identify the decidual environmental factor(s) that, when  
120 lacking in culture, trigger the dM polarization switch and enhance susceptibility to  
121 HIV-1 infection. IFN- $\gamma$ , present in the decidua, is one of the most potent stimuli of  
122 endogenous M1 macrophage activation and play a crucial role in immune responses  
123 against pathogens and in tumour immunosurveillance<sup>17</sup>. We thus investigated  
124 whether IFN- $\gamma$  affect dM plasticity and susceptibility to HIV-1 infection.

125 IFN- $\gamma$  treatment immediately after dM purification attenuated the increase in M2  
126 marker expression on day 7, as illustrated by CD163 and CD206 expression in  
127 (Figures 3a and 3b). In addition, no morphological change occurred when IFN- $\gamma$  was  
128 added to the culture medium (Supplementary figure S2b). Seven days of IFN- $\gamma$   
129 treatment restored IRF5 expression to the level found in freshly purified dM (Figure  
130 3c). In parallel, M1 markers (CD64, CD80, CD86) were strongly upregulated by IFN- $\gamma$   
131 (Figure 3d). However, CD4, CCR5 and DC-SIGN expression on IFN- $\gamma$ -treated dM  
132 varied greatly among donors (Figure 3e). Significantly lower IL-10 and IL-1RA  
133 secretion (Figure 3f) and higher chemokine secretion (CCL3, CCL4 and CCL5)  
134 (Figure 3g) were detected on day 7 of IFN- $\gamma$  treatment. Thus, 7 days of IFN- $\gamma$   
135 treatment restored certain features of freshly purified dM (cell morphology, M2

136 markers and IRF5 expression) and induced certain features of M1 macrophages (M1  
137 markers and low IL-10 and IL-1RA secretion).

138 To determine whether IFN- $\gamma$  treatment affected HIV-1 permissivity, purified dM  
139 were challenged with HIV-1/VSV-G on day 7 of culture with and without IFN- $\gamma$  (Figure  
140 4a). IFN- $\gamma$  impaired HIV-1 replication by more than 80%. This effect was not due to  
141 cytotoxicity (Supplementary figure S3a). IFN- $\gamma$  treatment also impaired dM infection  
142 by HIV-1<sub>BaL</sub>, as shown by p24 Ag quantification in the culture supernatant (Figure  
143 4b). By comparison with freshly purified dM, HIV-1 replication was also strongly  
144 inhibited in dM (IFN- $\gamma$ ) (Figures 4a and 4c).

145 Together, these results suggest that IFN- $\gamma$  participates in dM differentiation and  
146 contributes to the low permissivity of freshly purified dM to HIV-1 infection.

147

#### 148 **HIV-1 infection of dM (IFN- $\gamma$ ) is inhibited at the reverse-transcription and** 149 **integration steps**

150 As freshly purified dM rapidly switch to an M2 profile and become more  
151 susceptible to infection in cytokine-free culture, we used dM (IFN- $\gamma$ ), which recover  
152 characteristics of freshly purified dM, to investigate the mechanisms underlying the  
153 low permissivity of decidual macrophages.

154 Late reverse transcripts (U5GAG) and integrated proviral DNA that accumulated  
155 during the first 48 h of infection by HIV-1/VSV-G in dM (IFN- $\gamma$ ) were quantified and  
156 compared to those found in infected dM (US). IFN- $\gamma$  treatment led to markedly lower  
157 levels of U5GAG (Figure 5a) and integrated HIV-1 (Figure 5b). This strongly  
158 suggests that HIV-1 infection in dM (IFN- $\gamma$ ) is restricted at early post-entry steps of  
159 the replicative cycle.

160

161 **Expression of the cyclin-dependent kinase inhibitor p21Cip1/Waf1 (p21)**  
162 **correlates with IRF5 expression and restricts HIV-1 replication in dM (IFN- $\gamma$ )**

163 We then sought to identify the cellular factor(s) responsible for inhibiting the  
164 reverse transcription and integration steps. IFN- $\gamma$  and IFN- $\gamma$ -induced factors such as  
165 IRF5 are known to modulate the expression of genes involved in cell cycling and  
166 apoptosis. We focused on p21, because it has been reported to inhibit HIV-1  
167 replication in macrophages<sup>18-20</sup>.

168 First, we determined p21 expression by western blot in freshly isolated dM and dM  
169 (US) at day 7. Freshly purified dM expressed higher levels of p21 (Figure 6a). Next,  
170 we analyzed p21 expression in dM (US) and dM (IFN- $\gamma$ ) at day 7 (Figure 6b). p21  
171 was expressed significantly more strongly in dM (IFN- $\gamma$ ) than in dM (US), and  
172 correlated with strong IRF5 expression (Figure 6c). p21 expression was then  
173 knocked down by short interfering RNA (siRNA) in dM (IFN- $\gamma$ ) prior to challenge with  
174 HIV-1/VSV-G (Figure 6d). As a control, we used dM (US) and dM (IFN- $\gamma$ ) treated with  
175 random siRNA. p21 silencing in dM (IFN- $\gamma$ ) significantly increased U5GAG levels  
176 (Figure 6e) and also the numbers of integrated viral copies (Figure 6f) by comparison  
177 with dM (IFN- $\gamma$ ) treated with control siRNA. The resulting levels were not significantly  
178 different from those of control dM (US) (Figures 6e and 6f). p21 siRNA had no  
179 significant cytotoxic effect, and viability was similar in the three conditions (data not  
180 shown). These results show that p21 restricts HIV-1 reverse transcription and  
181 integration in dM (IFN- $\gamma$ ).

182 Interestingly, freshly purified dM and dM (IFN- $\gamma$ ) expressed higher levels of p21,  
183 than dM (US) (Figure 6a and 6b), suggesting that the increased dM susceptibility to  
184 HIV-1 infection in culture is probably associated with a decrease in p21 expression  
185 and that IFN- $\gamma$  addition to the culture medium of freshly purified dM restores both p21

186 expression and low permissivity to infection. Together, these findings suggest that  
187 p21 is involved in the control of HIV-1 replication in decidual tissue.

188

189 **TLR7/8 triggering does not alone induce dM polarization towards an M1 or M2**  
190 **profile but transiently blocks HIV-1 replication**

191 We have previously shown that dM express functional TLR7/8. We wondered  
192 whether these receptors, if activated after HIV-1 sensing, could influence dM  
193 polarization and reduce dM susceptibility to infection, as shown for monocytes and  
194 MDM<sup>11-14</sup>.

195 We first checked whether dM stimulation by a specific agonist (R848) that mimics  
196 HIV-1 recognition by TLR7/8 induced a dM polarization switch. dM were treated with  
197 R848 immediately after purification or left untreated. TLR7/8 triggering transiently  
198 increased CD163 expression on dM after 3 days of R848 treatment, while CD206  
199 and M1 expression fell gradually (Figures 7a and 7b). TLR7/8 engagement also  
200 down-regulated CD4, CCR5 and DC-SIGN expression (Figure 7c). TLR7/8 triggering  
201 by R848 did not induce morphological changes in culture, by comparison to dM (US)  
202 (data not shown). Moreover, IRF5 expression was down-regulated in R848-treated  
203 dM (Figure 7d). These changes were accompanied by higher IL-10 release by R848-  
204 stimulated dM compared to unstimulated dM, whereas IL-1RA secretion was not  
205 modified (Figure 7e). Together, these findings show that TLR7/8 activation by itself is  
206 not sufficient to fully polarize dM towards an M1 or M2 profile.

207 We then assessed the capacity of R848-stimulated dM to support HIV-1 infection.  
208 dM were treated with R848 directly after purification or left untreated, then challenged  
209 with HIV-1/VSV-G pseudotyped HIV-1 after 3 days (Figure 8a) or 7 days (Figure 8b)  
210 of culture. TLR7/8 triggering impaired HIV-1 replication after 3 days of stimulation,

211 but this antiviral effect had been lost by day 7 (Figure 8c). The inhibitory effect of  
212 R848 on HIV-1 replication was not due to cytotoxicity, as viability was unaffected  
213 (Supplementary figure S3b). TLR7/8-treated dM were also able to control HIV-1<sub>BaL</sub>  
214 infection, as shown by p24 Ag quantification in the culture supernatant (Figure 8d).  
215 We also found that TLR7/8 activation led to accumulation of late RT products (Figure  
216 8e) and to a marked decrease in integrated HIV-1 (Figure 8f). These results were  
217 consistent with the unmodified p21 expression upon TLR7/8 activation, by  
218 comparison to unstimulated dM (data not shown).

219 Together, these results show that TLR7/8 stimulation of dM leads to significant but  
220 transient inhibition of HIV-1 replication, after the reverse transcription step and before  
221 or at the integration step, potentially reinforcing the low permissivity of dM.

222

### 223 **TLR7/8 triggering in decidual explants induces M1 polarization of dM and** 224 **restricts HIV-1 replication**

225 We have previously shown that TLR7/8 triggering in dNK cells induces IFN- $\gamma$  and  
226 TNF- $\alpha$  secretion, which could potentially influence dM polarization and HIV-1  
227 permissivity<sup>3</sup>.

228 Therefore, to determine whether TLR7/8 stimulation can indirectly promote dM  
229 polarization, we stimulated cultured decidual explants with R848. Cytokine secretion  
230 by R848-treated and untreated explants was measured. Secretion of IFN- $\gamma$  and of  
231 IFN- $\gamma$ -induced cytokines such as CXCL9 and TNF- $\alpha$  was increased in R848-treated  
232 explants (Figure 9a), as was the secretion of both M1 (IL-1 $\beta$  and IL-12) (Figure 9b)  
233 and M2 cytokines (IL-1RA and IL-10) (Figure 9c). Secretion of chemokines (CCL3,  
234 CCL4 and CCL5) was also increased in R848-treated explants (Figure 9d). To further  
235 investigate the effect of TLR7/8 stimulation on dM polarization, decidual explants

236 were digested and the resulting cell suspensions were analyzed by flow cytometry.  
237 Untreated and IFN- $\gamma$ -treated explants were used as negative and positive controls,  
238 respectively. TLR7/8 triggering down-regulated the M2 marker CD206 (Figure 9e) as  
239 well as HIV-1 receptors and co-receptors (Figure 9f) on the dM surface, and  
240 enhanced M1 marker expression (CD64, CD80 and CD86) (Figure 9g). This  
241 phenotype modulation was similar to but less marked than that observed with IFN- $\gamma$ -  
242 treated explants.

243 Finally, we checked whether R848-treated explants controlled HIV-1 replication, by  
244 adding a TLR7/8 agonist to the explants prior to challenge with HIV-1<sub>BaL</sub>. HIV-1<sub>BaL</sub>  
245 infection was consistently inhibited in TLR7/8-stimulated explants, as shown by p24  
246 Ag measurement (Figure 9h). The viability of R848-treated explants was similar to  
247 that of untreated controls (data not shown).

248 TLR7/8 stimulation of decidual explants thus induced dM polarization toward an  
249 M1 profile and markedly inhibited HIV-1<sub>BaL</sub> infection.

## 250 Discussion

251

252 We report for the first time that mucosal macrophages from the *decidua basalis*  
253 are characterized by considerable plasticity in their local environment that determine  
254 their permissivity to HIV-1 infection.

255 dM have an M2-like phenotype but share features of both M1 (CD64, CD80, CD86  
256 and IRF5 expression) and M2 macrophages (CD163 and CD206 expression, IL-1RA  
257 and IL-10 secretion). We found that, in culture without exogenous cytokines, dM  
258 switched towards a more M2 profile. Thus, dM are likely predestined to adopt an M2  
259 program, which is ideally suited to homeostatic remodeling, angiogenesis and  
260 tolerogenesis during pregnancy. This is supported here by the observed IL-1RA and  
261 IL-10 secretion by dM cultured without exogenous stimuli. IL-10 may play an  
262 autocrine/paracrine role in the M2 polarity switch during dM culture <sup>16</sup>. IFN- $\gamma$   
263 treatment attenuated the increase in M2 marker expression and restored IRF5  
264 expression to the level observed in freshly purified dM, suggesting that the presence  
265 of IFN- $\gamma$  in decidual tissue participates in dM differentiation. However, IFN- $\gamma$   
266 treatment also induced other features of M1 macrophages, such as strong  
267 expression of CD64, CD80 and CD86 and weak secretion of IL-10 and IL-1RA. In  
268 contrast, it failed to increase IL-12 secretion, in keeping with reports that additional  
269 stimuli are needed to induce IL-12 secretion <sup>21,22</sup>. The combined M1 and M2  
270 signatures of freshly purified dM are probably ensured by several decidual factors in  
271 addition to IFN- $\gamma$ . In particular, contacts with decidual stromal and mesenchymal cells  
272 can induce some M2 features <sup>23</sup>. Phagocytosis of trophoblastic debris generated  
273 during pregnancy can also deviate dM toward an M2 phenotype, reducing CD80 and  
274 CD86 surface expression and inducing IL-10 and IL-1RA secretion <sup>24</sup>. The balance

275 between these different environmental signals likely accounts for the unique  
276 phenotype of freshly purified dM.

277 In parallel to the polarization changes observed in cytokine-free culture, we found  
278 that freshly purified dM became more permissive to HIV-1 infection over time. Only  
279 CCR5 expression increased significantly over time, possibly playing a role in the  
280 increased susceptibility to HIV-1<sub>BaL</sub> infection, but this would not explain why dM  
281 became more sensitive to infection by HIV-1/VSV-G, which does not require the  
282 presence of HIV-1 receptors.

283 IFN- $\gamma$  treatment of dM in culture restored the low permissivity of freshly purified  
284 dM, strongly inhibiting the HIV-1 reverse transcription and integration steps. R5 HIV-1  
285 entry might also be blocked, as CCR5-binding chemokines (CCL3, CCL4, and CCL5)  
286 are strongly induced by IFN- $\gamma$ <sup>25</sup>.

287 Thus, our data demonstrate that dM polarization status is responsible for the low  
288 permissivity to HIV-1 infection.

289 As freshly purified dM switch rapidly to an M2 profile in cytokine-free culture, and  
290 as IFN- $\gamma$  prevents this switch (in terms of the phenotype and resistance to infection),  
291 we used IFN- $\gamma$ -treated dM to examine the mechanisms underlying the low  
292 permissivity of freshly purified dM, and found that p21 inhibited the reverse  
293 transcription and integration steps. This is consistent with a previous study showing  
294 that IRF5 modulates the expression of growth-regulating and pro-apoptotic genes,  
295 including p21<sup>18</sup>. However, we cannot exclude the possibility that other IFN- $\gamma$ -induced  
296 genes may modulate p21 expression<sup>20</sup>. We also found that IFN- $\gamma$  treatment restored  
297 p21 expression in culture to a level similar to that of freshly purified dM, suggesting  
298 that p21 is involved in HIV-1 restriction in decidual tissue. p21 is known to restrict  
299 HIV-1 replication in macrophages either by inhibiting dNTP biosynthesis through a

300 RNR2-dependent pathway <sup>26</sup> or by modulating the phosphorylation of SAMHD1, a  
301 host restriction factor <sup>27</sup>. We have previously shown that the SAMHD1 pathway is  
302 involved in controlling HIV-1 infection of freshly purified dM <sup>8</sup>. RNR2 was  
303 undetectable in dM (IFN- $\gamma$ ), and SAMHD1 phosphorylation was slightly lower in dM  
304 (IFN- $\gamma$ ) than in controls, whereas the total SAMHD-1 level remained unchanged  
305 (preliminary data not shown). Thus, in decidual tissue, p21 might act through the  
306 SAMHD1 pathway.

307 Contrary to IFN- $\gamma$ , TLR7/8 triggering alone did not induce an M1 or M2 switch.  
308 However, TLR7/8 triggering impaired HIV-1/VSV-G infection and resulted in  
309 accumulation of late RT products, together with a marked reduction in the amount of  
310 integrated proviral DNA. These findings corroborate reports that TLR7/8 ligation  
311 impairs HIV-1 infection of monocytes and MDM <sup>12-14,28</sup>. However, as in previous  
312 studies <sup>11,29</sup>, we found no correlation between the TLR7/8-induced antiviral effect and  
313 IFN- $\alpha$  secretion, which was undetectable (data not shown). TLR7/8 engagement  
314 down-modulated CD4, CCR5 and DC-SIGN expression and induced secretion of  
315 CCR5-binding chemokines <sup>3</sup>, which are reported elsewhere to inhibit HIV-1 entry <sup>30</sup>.

316 The observed antiviral effects peaked 3 days after TLR7/8 activation and then  
317 declined, while the IFN- $\gamma$ -induced antiviral effect was more profound. This difference  
318 was probably due to differential IL-10 secretion by R848- and IFN- $\gamma$ -treated dM.  
319 Indeed, TLR activation induces factors such as IL-10 that restrain TLR-induced  
320 inflammatory activation and tissue damage. This inhibitory feedback also seems to  
321 control the TLR7/8-induced antiviral effect described above. By contrast, IFN- $\gamma$   
322 suppresses IL-10 secretion and the IL-10-dependent gene expression that regulate  
323 IFN- $\gamma$  responses. IFN- $\gamma$  signaling also induces proteins of the IRF family, which in  
324 turn generate a second wave of IFN- $\gamma$  target gene transcription <sup>31</sup>.

325 TLR7/8 triggering in purified dM failed to promote an M1 switch. In contrast,  
326 TLR7/8 triggering in decidual explants drove dM towards an M1 profile and  
327 consistently inhibited HIV-1<sub>BaL</sub> infection. This M1 switch can be attributed, at least in  
328 part, to the increased production of IFN- $\gamma$  and TNF- $\alpha$  by dNK cells upon TLR7/8  
329 activation. Cellular contacts with other decidual cells and other factors induced by  
330 TLR7/8 stimulation could also be involved in this switch. Indeed, IL-12 secretion,  
331 another hallmark of M1 polarization<sup>4</sup>, was also increased in R848-treated explants.  
332 This increase could reinforce the dM polarity switch by enhancing dNK secretion of  
333 IFN- $\gamma$ <sup>32</sup>. IL-12-related mechanisms and contacts between dM and dNK cells can also  
334 favor the emergence or selection of a macrophage population less sensitive to HIV-1  
335 infection<sup>33</sup>. dM switching towards an M1 phenotype could also induce TLR7/8  
336 overexpression and thereby further reduce the permissivity of dM to HIV-1<sup>29</sup>. The  
337 durable anti-HIV-1 effect observed in decidual explants is probably due to a  
338 synergistic action of TLR7/8 activation and IFN- $\gamma$  secretion.

339 Mucosal inflammation in the FRT promotes HIV-1 transmission and chronic HIV-1  
340 disease<sup>34</sup>. TLR stimulation of other FRT mucosae such as the vaginal mucosa  
341 induces proinflammatory cytokine and type I interferon secretion by plasmacytoid  
342 dendritic cells (pDC), and enhances viral replication<sup>35</sup>. We found that TLR7/8-  
343 stimulated decidual explants increased the secretion of both anti-inflammatory (IL-  
344 1RA and IL-10) and pro-inflammatory cytokines (TNF- $\alpha$  and IL-1 $\beta$ ). The cytokine  
345 profile upon TLR7/8 activation was compatible with the pro/anti-inflammatory  
346 cytokine balance required to maintain pregnancy during initiation of an immune  
347 response to HIV-1<sup>3</sup>. This cytokine balance, together with the small number of pDCs  
348 and the lack of interferon type I expression in the decidua, may explain these  
349 discrepancies.

350 To conclude, our data support a model in which several inter-dependent factors  
351 mediate the weak permissivity of dM to HIV-1 infection during the first trimester of  
352 pregnancy (Figure 10). In fact, the decidual environment necessary for successful  
353 pregnancy is unfavorable to HIV-1 replication. At the maternofetal interface,  
354 macrophages acquire distinct phenotypic and functional properties directed by the  
355 pro/anti-inflammatory balance (IFN- $\gamma$ /TNF- $\alpha$  versus IL-10/IL1-RA) and by physical  
356 contact with decidual cells. dM therefore have low permissivity to HIV-1 infection.  
357 Shortly after infection, p21 blocks HIV-1 reverse transcription and integration. In  
358 parallel, TLR7/8, which recognize HIV-1 sequences, are activated and further reduce  
359 dM permissivity by adding an extra brake after the reverse transcription step and at  
360 or before the integration step. TLR7/8 triggering also induces  $\beta$ -chemokine secretion  
361 and down-regulates HIV-1 receptor and co-receptor expression, which may limit viral  
362 entry. In addition, TLR7/8 triggering induces IFN- $\gamma$  and TNF- $\alpha$  release from dNK. This  
363 favors an M1 switch of neighboring dM and increases p21 expression, thereby  
364 limiting infection of new cells. In parallel, TLR7/8 induce IL-1RA and IL-10 secretion,  
365 thereby damping inflammation and preserving the pregnancy (Figure 10).

366 In addition to underlining the role of dM differentiation in HIV-1 control, our findings  
367 open new avenues of research into the role of dM differentiation in reproductive  
368 immunology and implantation failure.

369 **Materials and Methods**

370

371 **Ethics statement**

372 All the donors in this study provided their written informed consent. The French  
373 Biomedicine Agency (n° PF508-013), Assistance Publique des Hôpitaux de Paris (n°  
374 VAL/2011/06-41/02) and the Biomedical Research Committee of Institut Pasteur,  
375 Paris, France (n° 2005.024) approved the study. The blood used for viral  
376 amplification on PBMC were obtained from adult healthy donors (Établissement  
377 Français du Sang (n°12/EFS/134 / n° HS2013-24916)). All blood donors signed  
378 informed consent allowing the use of their blood for research purpose.

379

380 **Human decidual tissue collection, dM isolation, and reagents**

381 Decidual tissues were obtained from healthy women undergoing voluntary  
382 termination of pregnancy during the first trimester (8 - 12 weeks of gestation). dM  
383 were purified by positive selection with anti-CD14 magnetic beads. dM purity was  
384 checked by flow cytometry and was 93% ± 3.8% (mean + SEM). dM were stimulated  
385 3 or 7 days prior to various assays with R848 at 5µg/ml for TLR7/8 activation and  
386 IFN-γ at 100ng/ml for dM polarization switch. Detailed procedures are described in  
387 the supplementary materials and methods.

388

389 **HIV-1 isolates and infection**

390 For single-round infectious challenge, we used HIV-1 particles (600 ng of p24 Ag/10<sup>6</sup>  
391 cells) containing the luc reporter gene and pseudotyped with the vesicular stomatitis  
392 virus G protein (HIV-1/VSV-G). The efficiency of infection was determined after 72 h  
393 by measuring luciferase activity in cell lysates with the Luciferase reagent. For

394 productive infection, HIV-1<sub>BaL</sub> was used at 10<sup>-3</sup> MOI. HIV-1<sub>BaL</sub> replication was  
395 measured by p24 Ag ELISA in culture supernatants. Detailed procedures are  
396 described in the supplementary materials and methods.

397

### 398 **Decidual explants**

399 Decidual tissues were cut into 0.3-cm<sup>2</sup> pieces. For flow cytometry, explants were  
400 placed on collagen sponge gels in 1.5 ml of medium/well/sponge/piece prior to  
401 stimulation with R848 or IFN- $\gamma$ . Decidual tissue and the sponge were minced,  
402 digested and filtered. The total cell population was analyzed by flow cytometry. For  
403 experiments with HIV-1<sub>BaL</sub>, explants were stimulated overnight with R848, then  
404 challenged with HIV-1<sub>BaL</sub> for 12 h. After several washes the explants were placed on  
405 collagen sponge gels. All experiments were performed in triplicate. Details are  
406 provided in the supplementary materials and methods.

407

### 408 **Flow cytometry of cell surface markers**

409 Detailed procedures are described in the supplementary materials and methods. In  
410 brief, adherent dM were detached from plastic plates by pipetting without scraping.  
411 Cells were then incubated with an FcR blocking reagent and stained with conjugated  
412 antibodies. Cell surface marker expression was determined with an LSRII 2-Blue 2-  
413 Violet 3-Red 5-Yelgr-laser configuration. The results were analyzed with FlowJo  
414 9.1.3. software. MFI (%) was calculated as the ratio of treated dM (IFN- $\gamma$ ) or R848-  
415 treated dM to the dM (US) control.

416

### 417 **Western blotting**

418 Details are provided in the supplementary materials and methods. Protein bands

419 intensity were quantified with Image J software 1.47V and normalized to the actin  
420 band. The protein band intensity was quantified with the Image J software 1,47V and  
421 normalized to the actin band. Ratios (protein / actin) were then compared between  
422 the different conditions. Fold changes of IRF5 and p21 expression were calculated by  
423 comparing the normalized value of IRF5 and p21 from the IFN- $\gamma$ -treated samples to  
424 the normalized value of IRF5 and p21 from the dM (US) control from the same donor.

425

### 426 **Cytokine quantification**

427 dM culture supernatants were harvested after 1, 3 or 7 days and stored at -80°C.  
428 Soluble factors were measured in a Luminex assay with the Human Cytokine 25-plex  
429 antibody bead kit as recommended by the manufacturer (Invitrogen, Saint Aubin,  
430 France).

431

### 432 **siRNA transfection**

433 Small interfering RNAs (siRNAs) were purchased from GE Healthcare Dharmacon  
434 (Buckinghamshire, UK). The siRNA against the p21 gene was on-target plus siRNA  
435 n.12, and had the following sequence: 5' AGA CCA GCA UGA CAG AUU U 3'.  
436 Control siRNAs (Ctrl) were a pool of four on-target plus nontargeting siRNAs. siRNA  
437 transfection was performed using INTERFERin kits (Polyplus Transfection, Illkirch-  
438 Graffenstaden, France). 50 nM sip21 or siCtrl was prediluted in 1 mL of Opti-MEM, to  
439 which 20  $\mu$ L of INTERFERin was added. The transfection mix was left at room  
440 temperature for 10 min and then incubated with dM at 37°C for 16 hours. Cell culture  
441 medium was next replaced by siRNA-free culture medium during 8 hours. The  
442 transfection mix was then added for additional 16 hours prior to Western Blot and  
443 infection by HIV-1/VSV-G. Ctrl siRNA was also added to dM (US).

444

#### 445 **HIV-1 DNA quantitative PCR (qPCR)**

446 Total DNA in HIV-1/VSV-G-infected dM was extracted 48 h postinfection. Quantitative  
447 real-time PCR analysis of late (U5GAG) forms of viral DNA was carried out as  
448 previously described <sup>19</sup>. Integrated HIV-1 DNA was quantified by real-time Alu-LTR  
449 nested PCR using primers and probes described elsewhere <sup>19</sup>. The amount of viral  
450 DNA was normalized to the endogenous reference albumin gene. Detailed  
451 procedures are described in supplementary materials and methods.

452

#### 453 **Viability test**

454 The fixable viability dye 329 eFluor 780 (eBiosciences, Paris, France) was used to  
455 determine the viability of freshly purified dM and unstimulated dM on day 7 of culture,  
456 as recommended by the manufacturer. On days 3 and 7 of culture, the viability of  
457 stimulated dM (IFN- $\gamma$  and R848) and unstimulated dM was also compared. No  
458 significant differences were found.

459

#### 460 **Statistical analyses**

461 Statistical analyses were done with GraphPad Prism software version 5.0f. When  
462 several groups ( $\geq 3$ ) were compared, a Kruskal–Wallis test was used. When this test  
463 was significant, two by two comparisons were conducted and a Bonferroni correction  
464 was applied. Otherwise the Mann-Whitney test and the Wilcoxon matched pairs test  
465 were used. Lines or bars represent the mean, and error bars indicate SEM. The  
466 figure legends show in parentheses the number of independent donors used in the  
467 experiments. P values  $< 0.05$  were considered significant (\* $p < 0.05$ , \*\* $p < 0.005$ , \*\*\* $p$   
468  $< 0.0005$ , \*\*\*\* $p < 0.0001$ ). (#) Represents the statistical comparison of MFI values

469 between stimulated and unstimulated dM at a given time point. (#p < 0.05, ##p <  
470 0.005, ###p < 0.0005, ####p < 0.0001).

471

## 472 **DISCLOSURES**

473 The authors declared no conflict of interest.

474

## 475 **Acknowledgments**

476 The authors thank Dr G Chaouat, A Saez-Cirion, G Pancino, J C Valle Casuso and P  
477 Lebouteiller for scientific discussions, D. Young for critical editing of the manuscript  
478 and Dr Y Madec for his advice for statistical analysis. We also thank all the women  
479 who gave their informed consent, AP-HP (Assistance Publique Hôpitaux de Paris),  
480 Anne Lebreton, Séverine Ballan and clinical personnel for providing the samples;  
481 PIRC (Pole Intégré de Recherche Clinique, Institut Pasteur) for help with regulatory  
482 aspects; and Centre d'Immunologie Humaine, Institut Pasteur, for Luminex assay.  
483 This work was supported by ANRS (H.E-C and H.Q financial support and grant  
484 #12165/13129), Sidaction (H.E-C and M.D financial support and grant # AI20-3-  
485 01671), the TOTAL Foundation, INSERM, and Institut Pasteur.

486 **References**

487

488 1 Chouquet, C., Burgard, M., Richardson, S., Rouzioux, C. & Costagliola, D.  
489 Timing of mother-to-child HIV-1 transmission and diagnosis of infection based  
490 on polymerase chain reaction in the neonatal period by a non-parametric  
491 method. *Aids* 11, 1183-1184 (1997).

492 2 Marlin, R. et al. Antigen-presenting cells represent targets for R5 HIV-1  
493 infection in the first trimester pregnancy uterine mucosa. *PLoS One* 4, e5971,  
494 doi:10.1371/journal.pone.0005971 (2009).

495 3 Duriez, M. et al. Human decidual macrophages and NK cells differentially  
496 express Toll-like receptors and display distinct cytokine profiles upon TLR  
497 stimulation. *Front Microbiol* 5, 316, doi:10.3389/fmicb.2014.00316 (2014).

498 4 Krausgruber, T. et al. IRF5 promotes inflammatory macrophage polarization  
499 and TH1-TH17 responses. *Nat Immunol* 12, 231-238, doi:10.1038/ni.1990  
500 (2011).

501 5 Biswas, S. K. & Mantovani, A. Macrophage plasticity and interaction with  
502 lymphocyte subsets: cancer as a paradigm. *Nat Immunol* 11, 889-896,  
503 doi:10.1038/ni.1937 (2010).

504 6 Martinez, F. O. & Gordon, S. The M1 and M2 paradigm of macrophage  
505 activation: time for reassessment. *F1000Prime Rep* 6, 13, doi:10.12703/P6-13  
506 (2014).

507 7 Cassetta, L. et al. M1 polarization of human monocyte-derived macrophages  
508 restricts pre and postintegration steps of HIV-1 replication. *Aids* 27, 1847-  
509 1856, doi:10.1097/QAD.0b013e328361d059 (2013).

510 8 Quillay, H. et al. Distinct Characteristics of Endometrial and Decidual  
511 Macrophages and Regulation of Their Permissivity to HIV-1 Infection by  
512 SAMHD1. *J Virol* 89, 1329-1339, doi:10.1128/JVI.01730-14 (2015).

513 9 Siewiera, J. et al. Human cytomegalovirus infection elicits new decidual  
514 natural killer cell effector functions. *PLoS Pathog* 9, e1003257,  
515 doi:10.1371/journal.ppat.1003257 (2013).

516 10 Heil, F. et al. Species-specific recognition of single-stranded RNA via toll-like  
517 receptor 7 and 8. *Science* 303, 1526-1529, doi:10.1126/science.1093620  
518 (2004).

519 11 Wang, X., Chao, W., Saini, M. & Potash, M. J. A common path to innate  
520 immunity to HIV-1 induced by Toll-like receptor ligands in primary human  
521 macrophages. *PLoS One* 6, e24193, doi:10.1371/journal.pone.0024193  
522 (2011).

523 12 Campbell, G. R. & Spector, S. A. Toll-like receptor 8 ligands activate a vitamin  
524 D mediated autophagic response that inhibits human immunodeficiency virus  
525 type 1. *PLoS Pathog* 8, e1003017, doi:10.1371/journal.ppat.1003017 (2012).

526 13 Nian, H. et al. R-848 triggers the expression of TLR7/8 and suppresses HIV  
527 replication in monocytes. *BMC Infect Dis* 12, 5, doi:10.1186/1471-2334-12-5  
528 (2012).

529 14 Sica, A. & Mantovani, A. Macrophage plasticity and polarization: in vivo  
530 veritas. *J Clin Invest* 122, 787-795, doi:10.1172/JCI59643 (2012).

531 15 Seledtsov, V. I. & Seledtsova, G. V. A balance between tissue-destructive and  
532 tissue-protective immunities: a role of toll-like receptors in regulation of

- 533 adaptive immunity. *Immunobiology* 217, 430-435,  
534 doi:10.1016/j.imbio.2011.10.011 (2012).
- 535 16 Mantovani, A., Biswas, S. K., Galdiero, M. R., Sica, A. & Locati, M.  
536 Macrophage plasticity and polarization in tissue repair and remodelling. *J*  
537 *Pathol* 229, 176-185, doi:10.1002/path.4133 (2013).
- 538 17 Schoenborn, J. R. & Wilson, C. B. Regulation of interferon-gamma during  
539 innate and adaptive immune responses. *Adv Immunol* 96, 41-101,  
540 doi:10.1016/S0065-2776(07)96002-2 (2007).
- 541 18 Barnes, B. J., Kellum, M. J., Pinder, K. E., Frisancho, J. A. & Pitha, P. M.  
542 Interferon regulatory factor 5, a novel mediator of cell cycle arrest and cell  
543 death. *Cancer Res* 63, 6424-6431 (2003).
- 544 19 Bergamaschi, A. et al. The CDK inhibitor p21Cip1/WAF1 is induced by  
545 FcgammaR activation and restricts the replication of human immunodeficiency  
546 virus type 1 and related primate lentiviruses in human macrophages. *J Virol*  
547 83, 12253-12265, doi:10.1128/JVI.01395-09 (2009).
- 548 20 Armstrong, M. J. et al. Interferon Regulatory Factor 1 (IRF-1) induces  
549 p21(WAF1/CIP1) dependent cell cycle arrest and p21(WAF1/CIP1)  
550 independent modulation of survivin in cancer cells. *Cancer Lett* 319, 56-65,  
551 doi:10.1016/j.canlet.2011.12.027 (2012).
- 552 21 Skeen, M. J., Miller, M. A., Shinnick, T. M. & Ziegler, H. K. Regulation of  
553 murine macrophage IL-12 production. Activation of macrophages in vivo,  
554 restimulation in vitro, and modulation by other cytokines. *J Immunol* 156,  
555 1196-1206 (1996).
- 556 22 Lombardelli, L. et al. HLA-G5 induces IL-4 secretion critical for successful  
557 pregnancy through differential expression of ILT2 receptor on decidual CD4(+)  
558 T cells and macrophages. *J Immunol* 191, 3651-3662,  
559 doi:10.4049/jimmunol.1300567 (2013).
- 560 23 Kim, J. & Hematti, P. Mesenchymal stem cell-educated macrophages: a novel  
561 type of alternatively activated macrophages. *Exp Hematol* 37, 1445-1453,  
562 doi:10.1016/j.exphem.2009.09.004 (2009).
- 563 24 Abumaree, M. H., Chamley, L. W., Badri, M. & El-Muzaini, M. F. Trophoblast  
564 debris modulates the expression of immune proteins in macrophages: a key to  
565 maternal tolerance of the fetal allograft? *J Reprod Immunol* 94, 131-141,  
566 doi:10.1016/j.jri.2012.03.488 (2012).
- 567 25 Marlin, R. et al. Decidual soluble factors participate in the control of HIV-1  
568 infection at the maternofetal interface. *Retrovirology* 8, 58, doi:10.1186/1742-  
569 4690-8-58 (2011).
- 570 26 Allouch, A. et al. p21-mediated RNR2 repression restricts HIV-1 replication in  
571 macrophages by inhibiting dNTP biosynthesis pathway. *Proc Natl Acad Sci U*  
572 *S A* 110, E3997-4006, doi:10.1073/pnas.1306719110 (2013).
- 573 27 Allouch, A. et al. Reply to Pauls et al.: p21 is a master regulator of HIV  
574 replication in macrophages through dNTP synthesis block. *Proc Natl Acad Sci*  
575 *U S A* 111, E1325-1326 (2014).
- 576 28 Buitendijk, M., Eszterhas, S. K. & Howell, A. L. Toll-like receptor agonists are  
577 potent inhibitors of human immunodeficiency virus-type 1 replication in  
578 peripheral blood mononuclear cells. *AIDS Res Hum Retroviruses* 30, 457-467,  
579 doi:10.1089/AID.2013.0199 (2014).
- 580 29 Schlaepfer, E., Rochat, M. A., Duo, L. & Speck, R. F. Triggering TLR2, -3, -4, -  
581 5, and -8 reinforces the restrictive nature of M1- and M2-polarized  
582 macrophages to HIV. *J Virol* 88, 9769-9781, doi:10.1128/JVI.01053-14 (2014).

- 583 30 Lehner, T. et al. Up-regulation of beta-chemokines and down-modulation of  
584 CCR5 co-receptors inhibit simian immunodeficiency virus transmission in non-  
585 human primates. *Immunology* 99, 569-577 (2000).
- 586 31 Hu, X., Chakravarty, S. D. & Ivashkiv, L. B. Regulation of interferon and Toll-  
587 like receptor signaling during macrophage activation by opposing feedforward  
588 and feedback inhibition mechanisms. *Immunol Rev* 226, 41-56,  
589 doi:10.1111/j.1600-065X.2008.00707.x (2008).
- 590 32 O'Donnell, M. A. et al. Role of IL-12 in the induction and potentiation of IFN-  
591 gamma in response to bacillus Calmette-Guerin. *J Immunol* 163, 4246-4252  
592 (1999).
- 593 33 Bellora, F. et al. The interaction of human natural killer cells with either  
594 unpolarized or polarized macrophages results in different functional outcomes.  
595 *Proc Natl Acad Sci U S A* 107, 21659-21664, doi:10.1073/pnas.1007654108  
596 (2010).
- 597 34 Joseph, T. et al. Induction of cyclooxygenase (COX)-2 in human vaginal  
598 epithelial cells in response to TLR ligands and TNF-alpha. *Am J Reprod  
599 Immunol* 67, 482-490, doi:10.1111/j.1600-0897.2011.01099.x (2012).
- 600 35 Wang, Y. et al. The Toll-like receptor 7 (TLR7) agonist, imiquimod, and the  
601 TLR9 agonist, CpG ODN, induce antiviral cytokines and chemokines but do  
602 not prevent vaginal transmission of simian immunodeficiency virus when  
603 applied intravaginally to rhesus macaques. *J Virol* 79, 14355-14370,  
604 doi:10.1128/JVI.79.22.14355-14370.2005 (2005).
- 605

606 **Figure legends**

607

608 **Figure 1. dM become more permissive to HIV-1 infection in cytokine-free**  
609 **culture.**

610 (a) Freshly purified dM were challenged with HIV-1/VSV-G at day 0, 3 and 7 of  
611 culture. HIV-1 replication was monitored by measuring luciferase activity (n=7).

612 (b) dM were challenged with HIV-1<sub>BaL</sub> immediately after isolation (day 0) or after 7  
613 days of cytokine-free culture. Viral production was followed by quantifying p24 Ag in  
614 the supernatant. p24 Ag production on day 21 post-infection (n=7).

615 Mean  $\pm$  SEM of *n* independent donors.

616

617 **Figure 2. dM switch towards a more M2 profile in cytokine-free culture.**

618 (a) Representative histograms of CD163 and CD206 expression on dM, as measured  
619 by flow cytometry.

620 (b) CD163 and CD206 mean fluorescent intensity (MFI) over time (n=6).

621 (c) CD4, CCR5 and DC-SIGN mean fluorescent intensity (MFI) on day 0 and on day  
622 7 of culture (n=6).

623 (d) Representative western blot of IRF5 expression by dM over time (left panel). The  
624 protein band intensity was quantified and normalized to the actin band. Ratio (IRF5 /  
625 actin) was then compared over time (right panel) (n=6).

626 (e) dM cytokine release after 1, 3 and 7 days of culture (n=6).

627 Mean  $\pm$  SEM of *n* independent donors.

628

629

630

631 **Figure 3. IFN- $\gamma$  addition to cultured dM restores partially the phenotype of**  
632 **freshly purified dM.**

633 (a) Representative histograms of IFN- $\gamma$ -induced modulation of CD163 and CD206  
634 expression on day 7, as measured by flow cytometry.

635 (b) IFN- $\gamma$ -induced change (%) in CD163 and CD206 expression (MFI) on dM  
636 compared to time-matched unstimulated dM (n=6).

637 (c) Representative western blot of IRF5 expression by IFN- $\gamma$ -stimulated and  
638 unstimulated dM on day 7 of culture (left panel). The protein band intensity was  
639 quantified and normalized to the actin band. Ratio (IRF5 / actin) was then compared  
640 between IFN- $\gamma$ -stimulated and unstimulated dM on day 7 of culture (right panel)  
641 (n=19).

642 (d) IFN- $\gamma$ -induced change (%) in CD64, CD80 and CD86 expression (MFI) on dM, as  
643 compared to time-matched unstimulated dM (n=6).

644 (e) IFN- $\gamma$ -induced changes (%) in CD4, DC-SIGN and CCR5 expression (MFI) on dM  
645 on day 7 of culture, by comparison with unstimulated dM (n=17).

646 (f) dM cytokine and (G)  $\beta$ -chemokine release after 7 days of culture (n=7).

647 Mean  $\pm$  SEM of *n* independent donors. # = statistical comparison of MFI values  
648 between IFN- $\gamma$ -stimulated dM versus unstimulated (US) dM at the same time.

649

650 **Figure 4. IFN- $\gamma$  addition to cultured dM restores the resistance to HIV-1.**

651 (a) Freshly purified dM and 7-day IFN- $\gamma$ -stimulated and unstimulated (US) dM were  
652 challenged with HIV-1/VSV-G. HIV-1 replication was monitored by measuring  
653 luciferase activity in cell lysates (n=13).

654 (b) IFN- $\gamma$  stimulated and US dM were challenged with HIV-1<sub>BaL</sub> on day 7 of culture.  
655 HIV-1 p24 Ag was measured by ELISA in the supernatants (n=6).

656 (c) p24 Ag production on day 21 after infection by HIV-1<sub>BaL</sub> was compared between  
657 freshly purified dM and 7-day IFN- $\gamma$ -stimulated or unstimulated dM (n=6).  
658 Mean  $\pm$  SEM of *n* independent donors.

659

660

661 **Figure 5. IFN- $\gamma$  restricts HIV-1 infection of dM at the reverse transcription and**  
662 **integration steps.**

663 7-day IFN- $\gamma$ -stimulated and unstimulated (US) dM were challenged with HIV-1/VSV-  
664 G. Late reverse-transcription products (U5GAG) (n=6) (a) and integrated forms (n=8)  
665 (b) were quantified by qPCR. Mean  $\pm$  SEM of *n* independent donors.

666

667 **Figure 6. p21 is involved in low dM permissivity to HIV-1.**

668 (a) Representative western blot of p21 expression by freshly purified dM (day 0) and  
669 by unstimulated dM at day 7 of culture (left panel). The protein band intensity was  
670 quantified and normalized to the actin band. Ratio (p21 / actin) was then compared  
671 between dM at day 0 and day 7 (right panel) (n=6).

672 (b) Representative western blot of p21 expression by IFN- $\gamma$ -stimulated and  
673 unstimulated (US) dM on day 7 of culture (left panel). Ratio (p21 / actin) was then  
674 compared between the 7-days IFN- $\gamma$ -stimulated and unstimulated (US) (right panel)  
675 (n=20).

676 (c) Fold changes of IRF5 and p21 expression were calculated by comparing the  
677 normalized value of IRF5 and p21 from the IFN- $\gamma$ -treated samples to the normalized  
678 value of IRF5 and p21 from the dM (US) control.

679 Correlation between fold changes in IRF5 and p21 expression on day 7 of IFN- $\gamma$   
680 treatment compared to time-matched unstimulated dM (n=19). Spearman's R value is

681 shown.

682 (d) Representative western blot of p21 expression in 7-day IFN- $\gamma$ -stimulated and  
683 unstimulated dM transfected with p21-specific siRNA or with an irrelevant control  
684 siRNA (Ctrl) (n=9).

685 (e) Number of late reverse transcription products (U5GAG) and (F) integrated forms  
686 in dM transfected with p21-specific or control siRNA (n=9).

687 Mean  $\pm$  SEM of *n* independent donors.

688

689 **Figure 7. TLR7/8 triggering is not sufficient to induce dM polarization towards**  
690 **an M1 or M2 profile.**

691 (a) % change in dM CD163 and CD206, (b) CD64, CD80 and CD86 expression (MFI)  
692 induced by R848 as compared to time-matched unstimulated dM.

693 (c) % change in dM CD4, DC-SIGN and CCR5 expression (MFI) induced by R848 as  
694 compared to time-matched unstimulated dM.

695 (d) Ratio of IRF5 to actin expression by R848-stimulated and unstimulated dM on  
696 days 3 and 7 of culture.

697 (e) dM cytokine release after 3 days of culture.

698 Mean  $\pm$  SEM of 6 independent donors. # = statistical comparison of MFI values  
699 between R848-stimulated versus unstimulated dM at the same time.

700

701 **Figure 8. TLR7/8 triggering restricts HIV-1 replication after the reverse**  
702 **transcription step and at or before the integration step.**

703 R848-stimulated and unstimulated (US) dM were challenged with HIV-1/VSV-G on  
704 day 3 (n=13) (a) or day 7 (n=6) (b) of culture. HIV-1 replication was monitored by  
705 measuring luciferase activity. The % of luciferase activity inhibition was determined

706 by comparison with time-matched unstimulated dM (c).  
707 (d) R848-stimulated and US dM were challenged with HIV-1<sub>BaL</sub> on day 3 of culture.  
708 HIV-1 p24 Ag was measured by ELISA in the culture supernatants (n=9)  
709 Late reverse transcription products (U5GAG) (n=8) (e) and integrated forms (n=8) (f)  
710 were quantified by qPCR in dM infected with HIV-1/VSV-G on day 3. Mean  $\pm$  SEM of  
711 *n* independent donors.

712

713

714 **Figure 9. TLR7/8 triggering in decidual explants induces M1 polarization of dM**  
715 **and restricts HIV-1 replication**

716 Decidual explants were stimulated with R848 or left unstimulated (US).  
717 (a) (b) (c) (d) cytokine and  $\beta$ -chemokine concentrations in explant supernatants after  
718 3 days of culture.  
719 (e) (f) (g) Marker expression on CD45<sup>+</sup> CD14<sup>+</sup> dM after explant digestion on day 7 of  
720 culture, as measured by flow cytometry of total decidual cells. The % change in MFI  
721 induced by R848 and IFN- $\gamma$  was determined by comparison with time-matched  
722 unstimulated explants.  
723 (h) Explants were stimulated with R848 or left untreated prior to challenge with HIV-  
724 1<sub>BaL</sub>. HIV-1 p24 Ag was measured by ELISA in explant supernatants.  
725 Mean  $\pm$  SEM of 7 independent donors. # = statistical comparison of MFI values  
726 between R848-stimulated versus unstimulated dM.

727

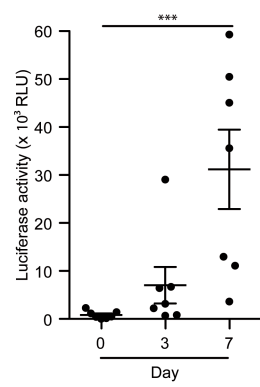
728 **Figure 10. Integrated model of the inter-dependent factors involved in dM**  
729 **differentiation and natural resistance to HIV-1 infection.**

730 In case of HIV-1 infection, p21 blocks HIV-1 replication at the reverse transcription

731 and integration steps (1). In parallel, TLR7/8 activation by HIV-1 sequences (2), add  
732 an extra brake after the reverse transcription step and at or before the integration  
733 step (3). TLR7/8 triggering may also limit viral entry by inducing  $\beta$ -chemokine  
734 secretion (4) and by down-regulating HIV-1 receptor and co-receptor expression (5).  
735 In addition, TLR7/8 triggering induces IFN- $\gamma$  and TNF- $\alpha$  release from dNK cells (6),  
736 which favors an M1 switch of neighboring dM (7) and increases p21 expression (8).  
737 In parallel, TLR7/8 induce IL-1RA and IL-10 secretion that restrain TLR-induced  
738 inflammatory activation and tissue damage (9). In conclusion, the decidual pro/anti-  
739 inflammatory cytokine balance shape the phenotype of dM and their permissivity to  
740 HIV-1 infection (10).

Figure 1

a



b

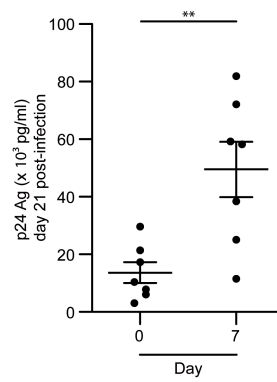


Figure 2

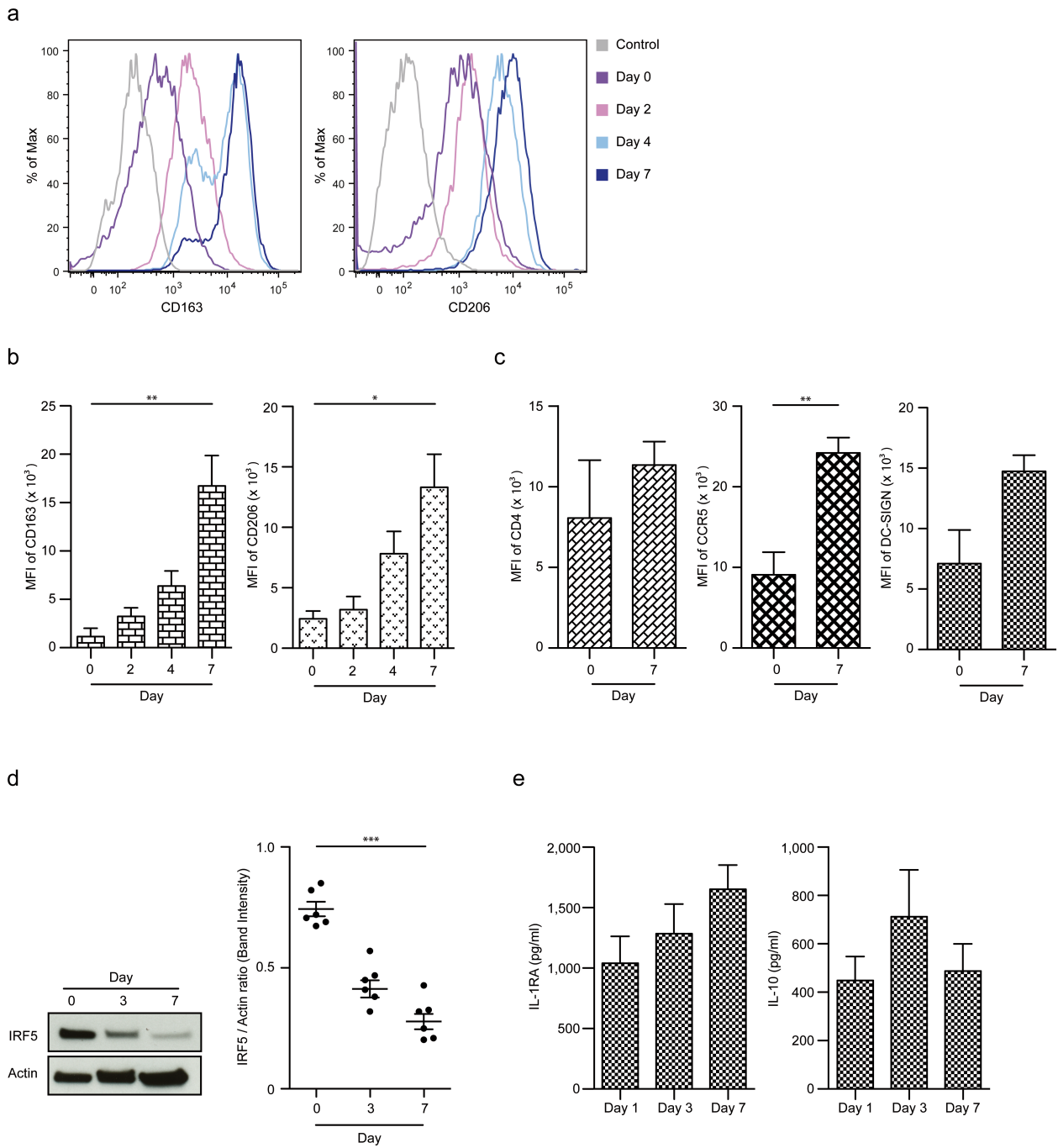


Figure 3

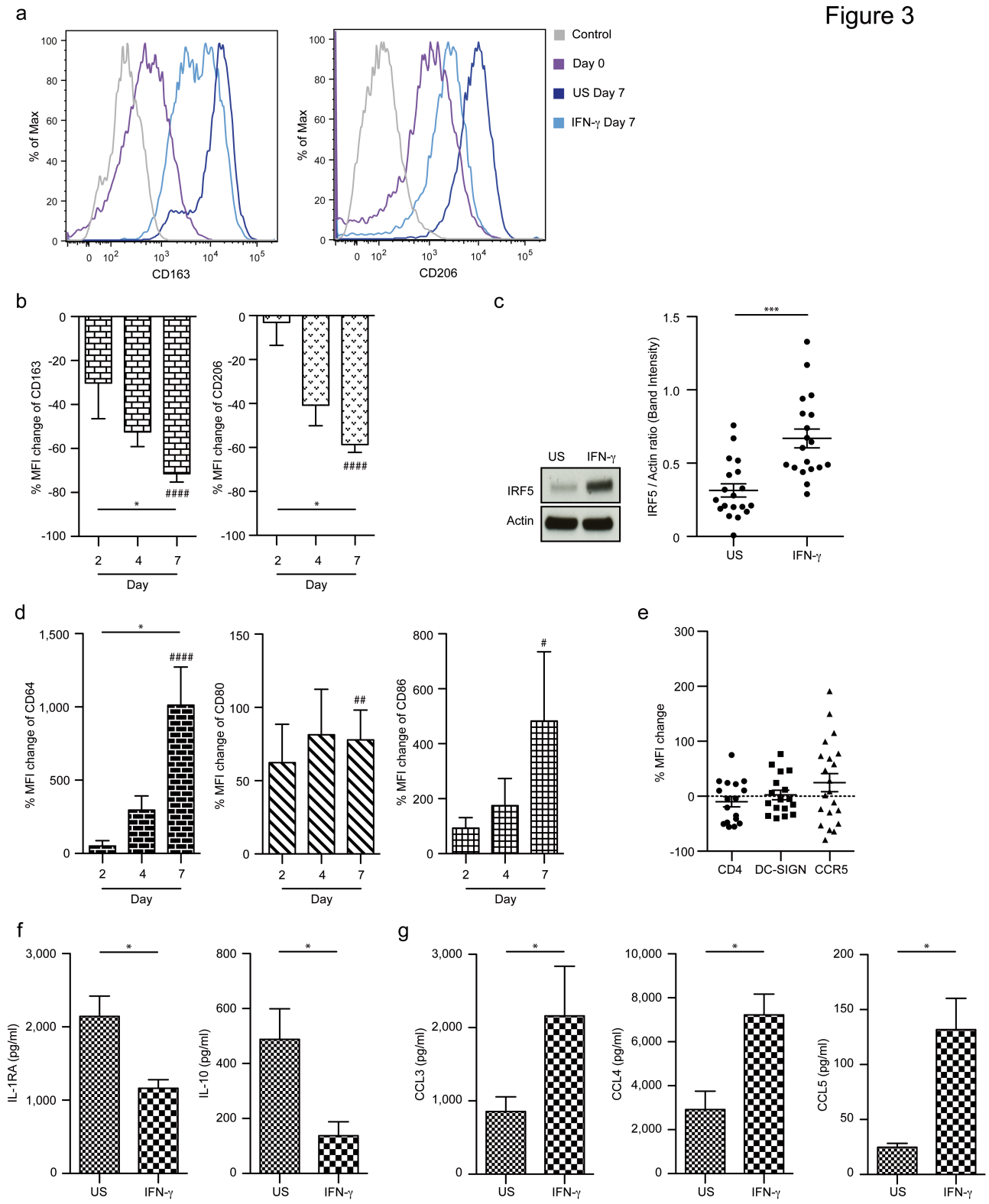
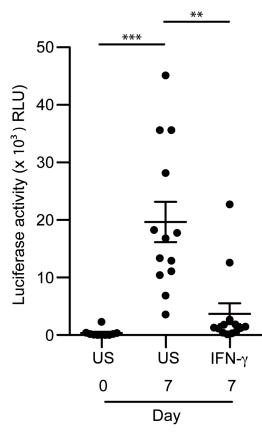
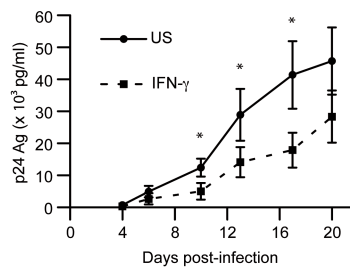


Figure 4

a



b



c

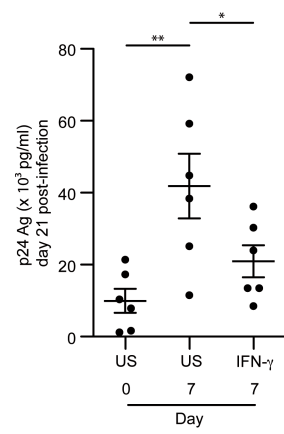


Figure 5

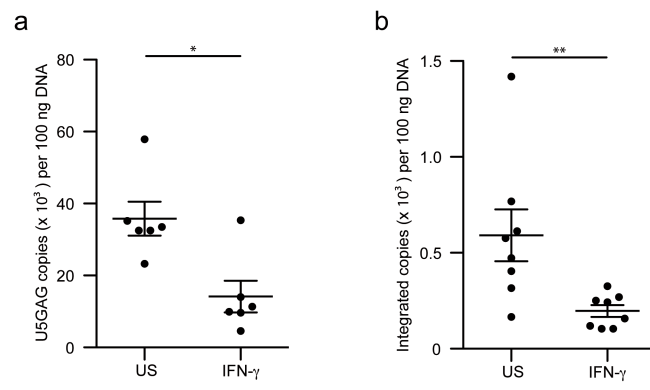


Figure 6

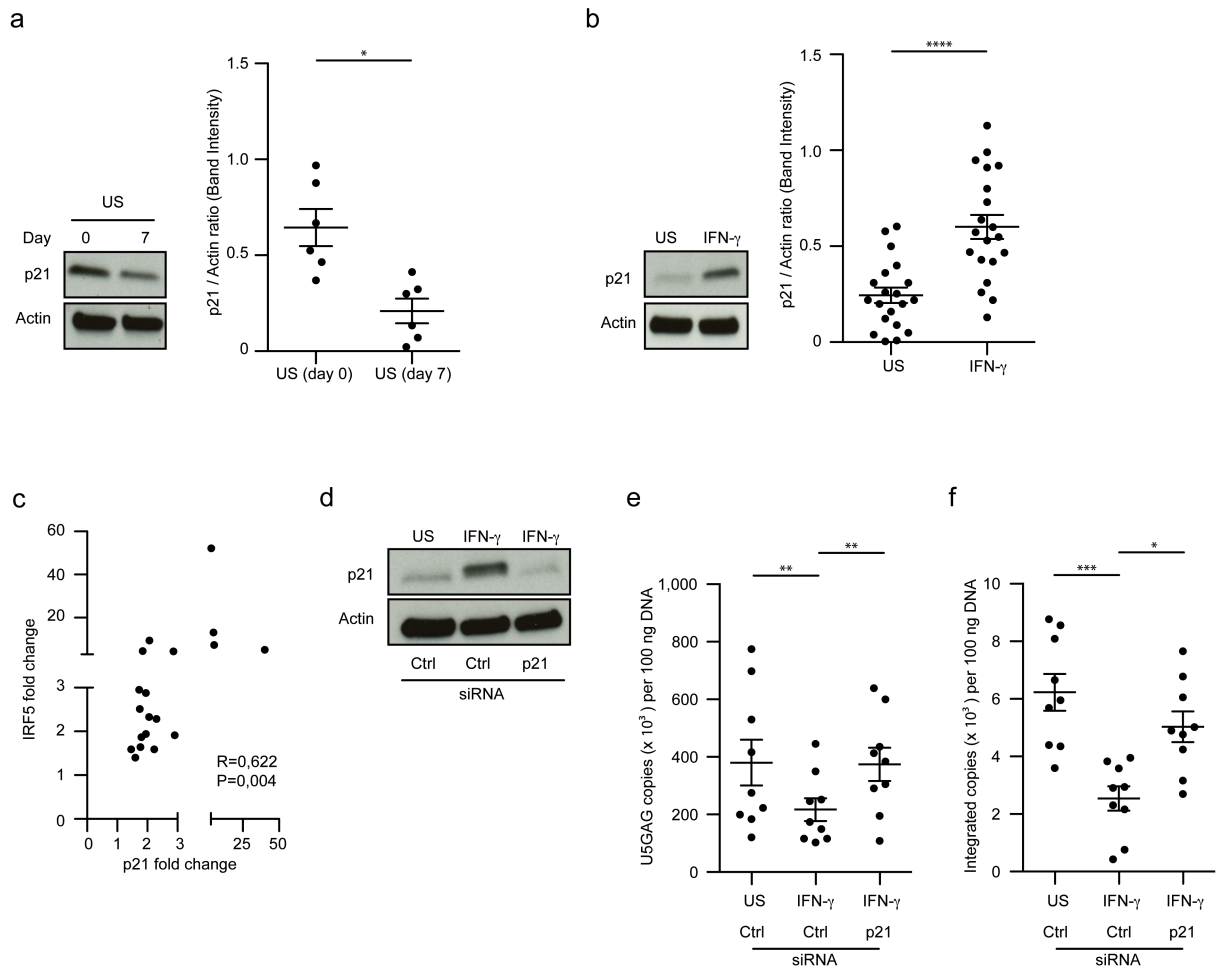


Figure 7

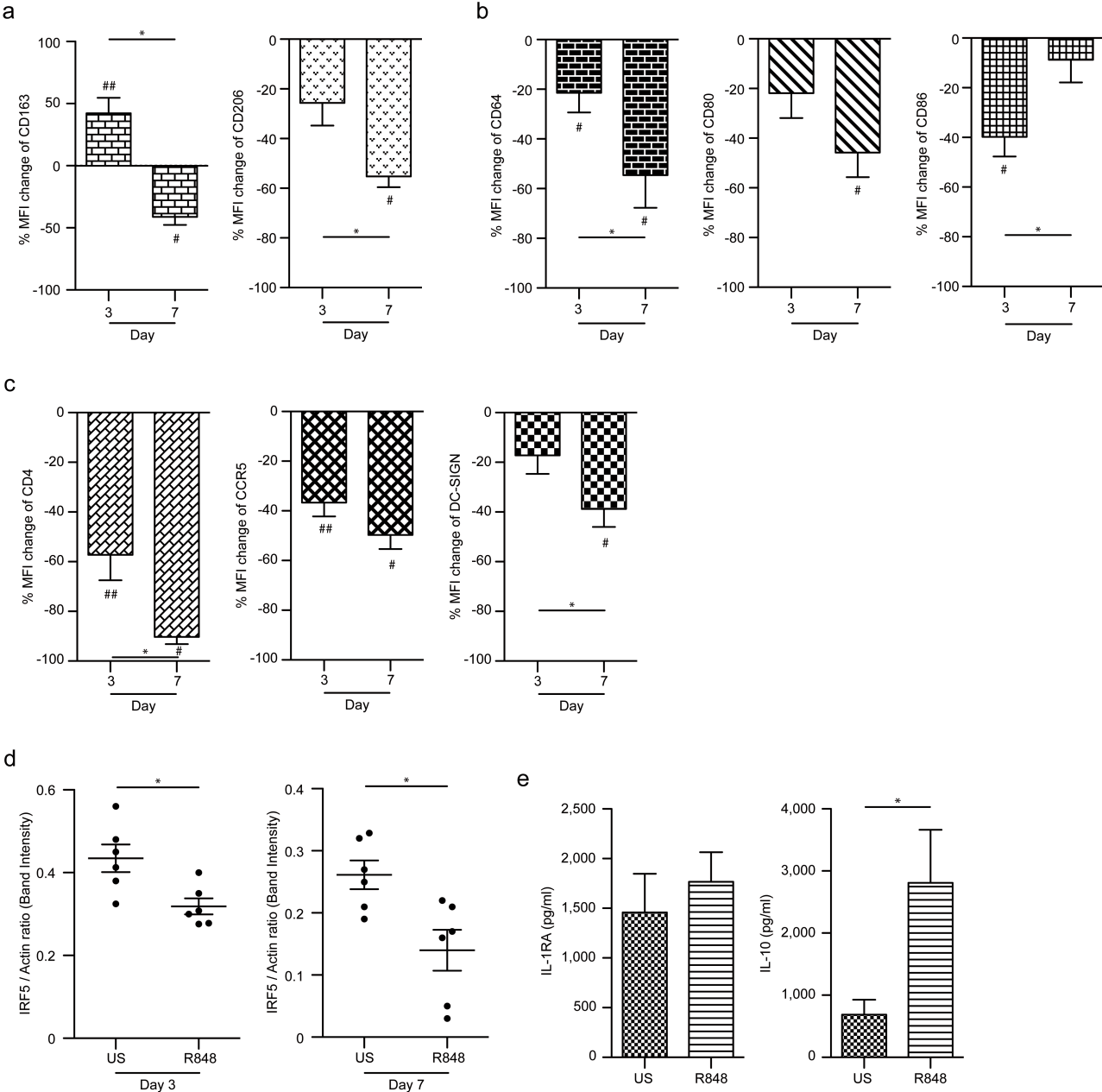
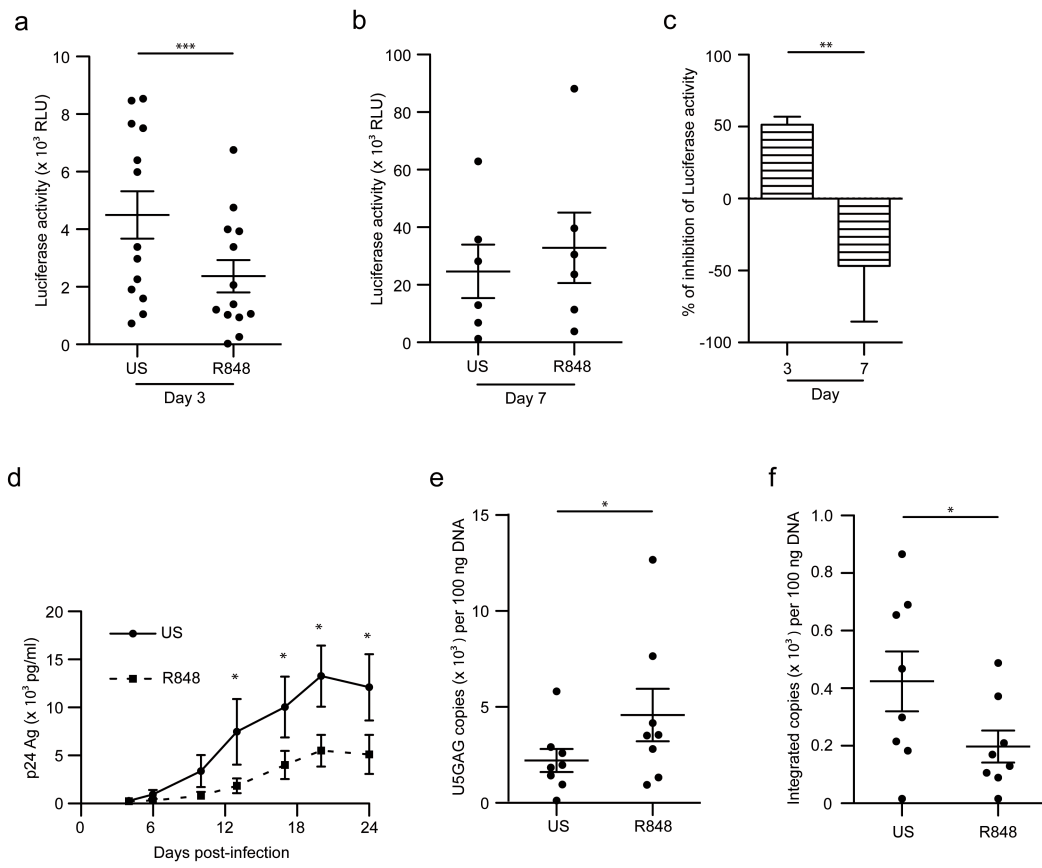


Figure 8



**Figure 9**

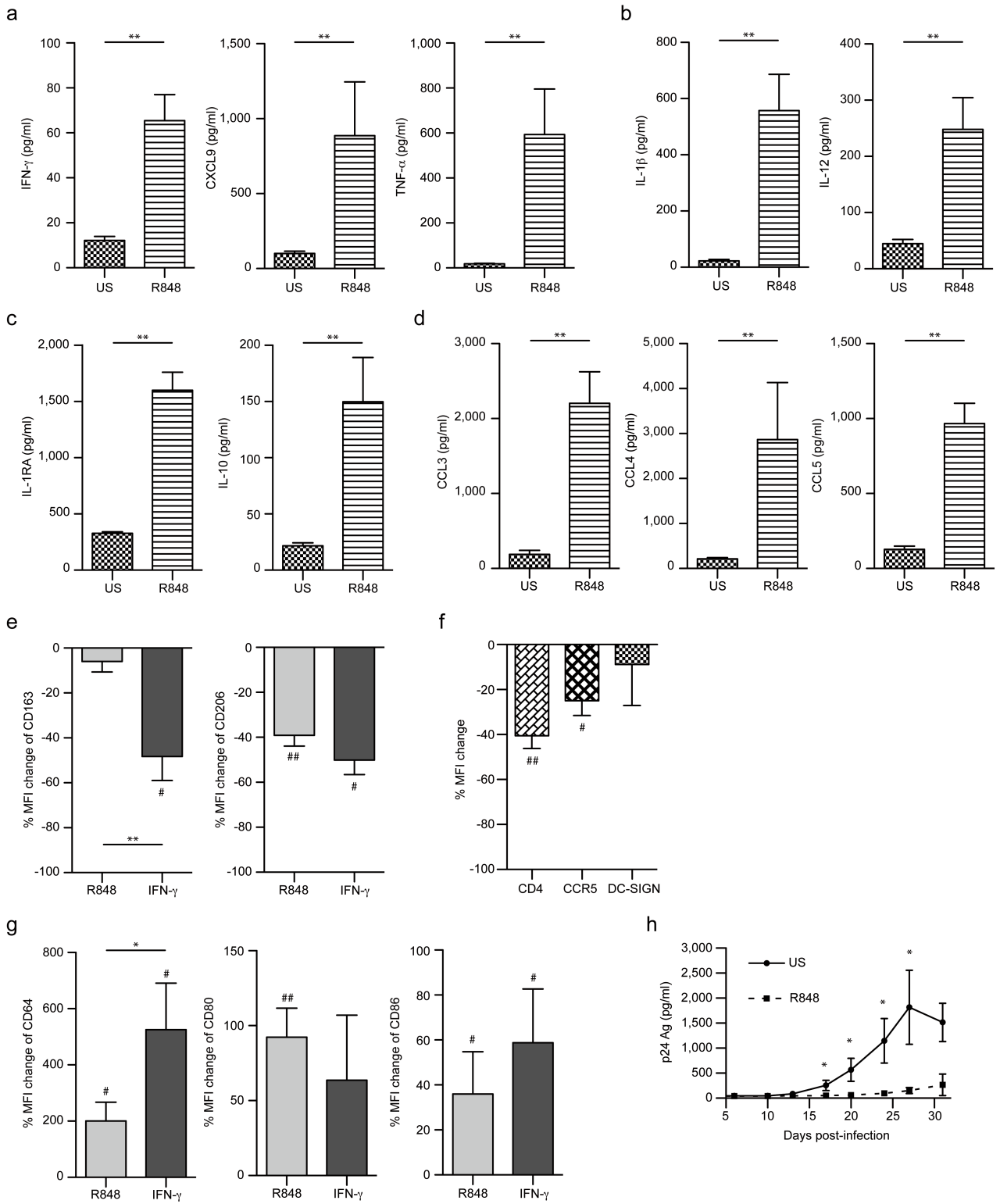
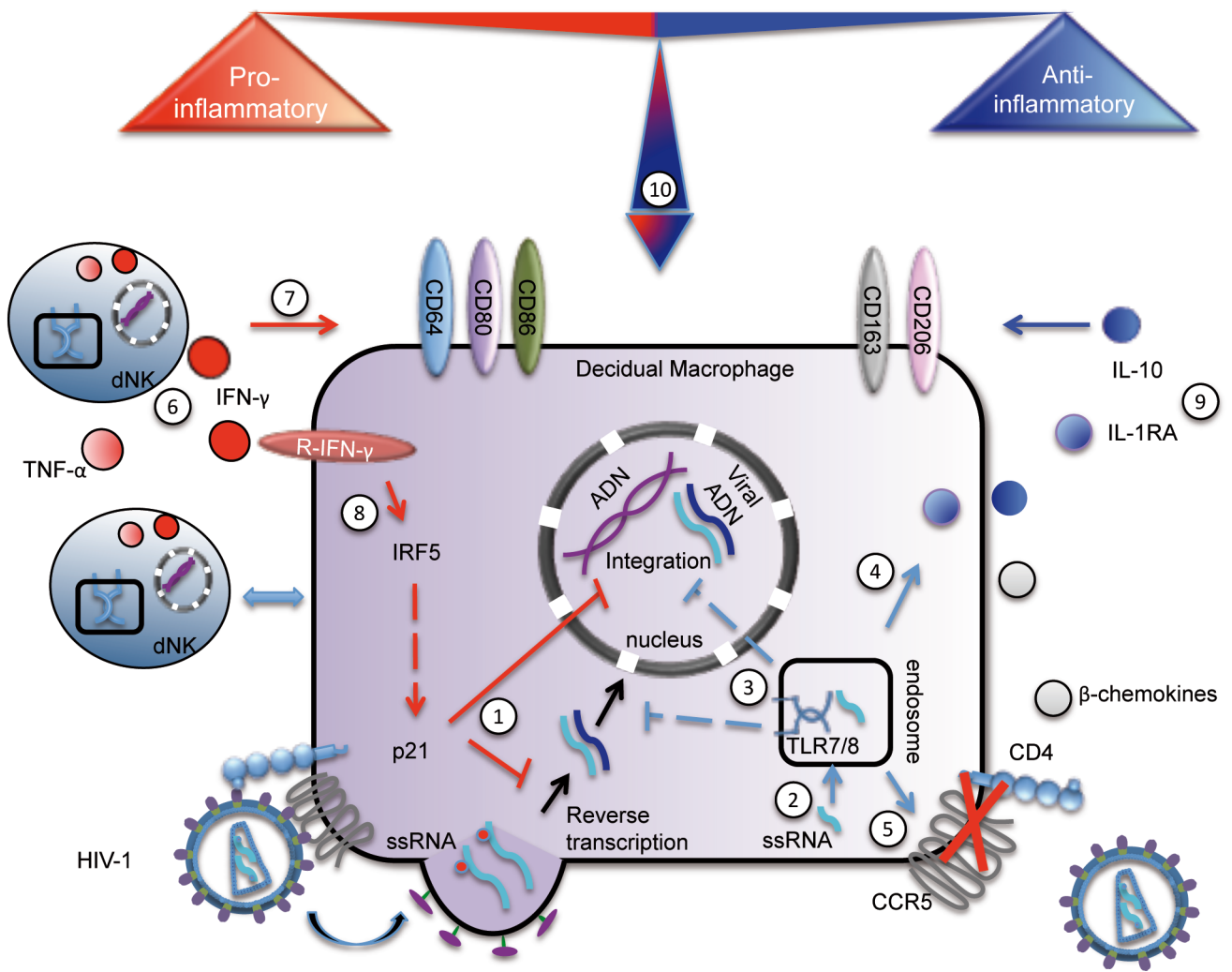


Figure 10



## **Supplementary figure legends**

### **Supplementary Figure S1. M1 marker expression on dM in cytokine-free culture.**

(a) (b) (c) CD64, CD80 and CD86 mean fluorescent intensity (MFI) over time. Mean  $\pm$  SEM of 6 independent donors.

### **Supplementary Figure S2. dM morphology in culture.**

Morphology of unstimulated (US) (a) and IFN- $\gamma$ -stimulated (b) dM on days 2 and 7 of culture.

Bars = 100  $\mu$ m. Original magnification X40.

### **Supplementary Figure S3. Viability of IFN- $\gamma$ - and R848-stimulated dM.**

(a) Viability of IFN- $\gamma$ -stimulated and unstimulated (US) dM after 7 days of culture, as measured by flow cytometry after labeling dead cells. A representative FACS dot plot gated on CD45<sup>+</sup> CD14<sup>+</sup> dM is shown.

(b) Viability of R848-stimulated and US dM after 3 days of culture, as measured by flow cytometry. A representative FACS dot plot gated on CD45<sup>+</sup> CD14<sup>+</sup> dM is shown.

## **Supplementary Materials and Methods**

### **Human decidual tissue collection, dM isolation, and reagents**

Decidual tissues were obtained from healthy women undergoing voluntary termination of pregnancy during the first trimester (8 - 12 weeks of gestation) at Antoine Béclère Hospital (Clamart, France) or Pitié-Salpêtrière Hospital (Paris,

France). After isolation, the decidua was minced and digested with 1 mg/mL collagenase IV (Sigma, St Quentin Fallavier, France) and 250 U/mL recombinant DNase I (Roche, Meylan, France) for 45 minutes at 37°C under agitation. The cell suspension was filtered successively through 100-, 70- and 40- $\mu$ m sterile nylon cell strainers (BD Biosciences, Le pont de Claix, France). Mononuclear cells were isolated from the cell suspension by Ficoll gradient centrifugation using Lymphocyte Separation Medium (PAA, Les Mureaux, France). dM were purified by positive selection using anti-CD14 magnetic beads (Miltenyi, Paris, France). Their purity was checked by flow cytometry and was 93%  $\pm$  3.8% (mean + SEM). Contaminating cells were mainly CD45<sup>-</sup> cells. dM were cultured at 2x10<sup>6</sup> cells/mL in HamF12 and DMEM Glutamax (Gibco, Cergy Pontoise, France) supplemented with 15% fetal calf serum (PAA), penicillin (0.1 U/mL) and streptomycin (10<sup>-8</sup> g/L). dM were stimulated for 3 or 7 days prior to various assays with R848 at 5  $\mu$ g/ml for TLR7/8 activation (Invivogen, Toulouse, France) and with IFN- $\gamma$  at 100 ng/ml for polarization switch studies (R&D, Lille, France).

### **HIV-1 isolates and infection**

For single-round infection, we used HIV-1 particles containing the luc reporter gene and pseudotyped with the vesicular stomatitis virus G protein (HIV-1/VSV-G). HIV1/VSV-G was produced by transient cotransfection of HEK293T cells with proviral pNL4-3 Nef<sup>-</sup> Env<sup>-</sup> Luc<sup>+</sup> DNA and the pMD2 VSV-G expression vector. Supernatants containing pseudotyped viruses were harvested 72 h after transfection, passed through 0.45- $\mu$ m pore-size filters and stored at - 80°C. The viral stocks were titrated on HeLa P4P cells. dM were spinoculated with the HIV-1/VSV-G pseudotype (600 ng of p24 Ag/10<sup>6</sup> cells) for 30 minutes at 1200 g then incubated at 37°C for 30

minutes. The efficiency of infection by the viral pseudotype was determined 72h later by luciferase assay in cell lysates, using the Luciferase reagent (Promega, Lyon, France) on a Glomax luminometer, according to the manufacturer's instructions. For productive infection, HIV-1<sub>BaL</sub> was used. HIV-1<sub>BaL</sub> was amplified for 11 days in PHA-stimulated PBMC depleted of CD8<sup>+</sup> cells, from three blood donors. The virus was concentrated by centrifugation on Vivaspin 100 000-Kda columns (Sartorius, Palaiseau, France) at 2000 g for 30 minutes, and was titrated on PBMC. dM were incubated for 1 hour with HIV-1<sub>BaL</sub> at 10<sup>-3</sup> MOI at 37°C. Culture supernatants were collected every 3 or 4 days and stored at -80°C. HIV-1BaL production was measured by ELISA (Zeptometrix, Franklin, Massachusetts, USA) measurement of the viral core antigen p24 (p24 Ag) in culture supernatants, according to the manufacturer's instructions.

### **Decidual explants**

Decidual tissues were cut into 0.3 cm<sup>2</sup> pieces. For flow cytometry, explants were placed on collagen sponge gels (Pfizer, Paris, France) in 1.5 ml of medium/well/sponge/piece prior to stimulation with R848 or IFN- $\gamma$ . The decidual tissue and sponge were then minced and digested with 1 mg/mL collagenase IV (Sigma, St Quentin Fallavier, France) and 250 U/mL recombinant DNase I (Roche, Meylan, France) for 20 minutes at 37°C under agitation. The cell suspension was filtered through 40- $\mu$ m sterile nylon cell strainers (BD Biosciences, Le pont de Claix, France). The total cell population was used for flow cytometry. Explants were stimulated overnight with R848 then infected with HIV-1<sub>BaL</sub> for 12h. After several washes, explants were placed on collagen sponge gels. Experiments were all performed in triplicate and the mean values are reported in the figures.

### **Flow cytometry of cell surface markers**

Adherent dM were washed with cold EDTA/PBS (2 mM) and detached from the plastic plates by pipetting without scraping. Cells were labeled with anti-CCR5 (APC-Cy7, clone 2D7, BD), anti-CD14 (Pacific Blue, clone 3.9, BD), anti-CD163 (PE, clone GHI/61, BD), anti-CD206 (APC, clone 19.2, BD), anti-CD4 (PE-Cy7, clone SK3, BD), anti-CD45 (Amcyan, clone 2D1, BD), anti-CD64 (FITC, clone 10.1, BD), anti-CD80 (PE, clone 307/4, BD), anti-CD86 (PE, clone 2331, BD), and anti-DC-SIGN (PE, clone 120507, R&D) (R&D, Lille, France). dM were incubated with an FcR blocking reagent (Miltenyi, Paris, France) before staining with the conjugated antibodies for 20 minutes at 4°C. After two EDTA/PBS washes, cells were fixed in 1% paraformaldehyde, and surface marker expression was determined with an LSRII 2-Blue 2-Violet 3-Red 5-Yelgr-laser configuration (BD Biosciences, Le pont de Claix, France). The results were analyzed with FlowJo 9.1.3. software (Tristar, Ashland, USA). MFI (%) was calculated as the ratio of treated dM (IFN- $\gamma$ ) or R848-treated dM to the unstimulated dM control.

### **Western blotting**

Freshly isolated dM or dM cultured in 48-well plates were washed with PBS then lysed in 120  $\mu$ L of lysis buffer (50 mM Tris·HCl, pH 7.4, 150 mM NaCl, 1 mM EDTA, and 1% TritonX-100) containing a protease and phosphatase inhibitor mixture (Roche, Meylan, France). Cell extracts (10–25  $\mu$ g) were hybridized with the primary antibodies, followed by secondary horseradish peroxidase anti-mouse (Cell Signaling, Leiden, Netherlands) or anti-rabbit (Sigma-Aldrich, Saint Louis, USA) antibodies. Proteins were revealed on Hyperfilms (Amersham, Velizy-Villacoublay,

France) by using the Pierce ECL western blotting substrate (Thermo Scientific, Waltham, USA). The following primary antibodies were used: anti-p21 (clone CP74, Merck Millipore, Fontenay sous Bois, France), anti-IRF5 (ab140593, abcam, Paris, France) and anti- $\beta$ -actin (clone AC-74, Sigma-Aldrich, Saint Louis, USA). Primary antibodies were all used at 1 :2000 dilution in 1% skimmed milk in PBS-0.05% Tween, except for anti- $\beta$ -actin (1 :10 000).

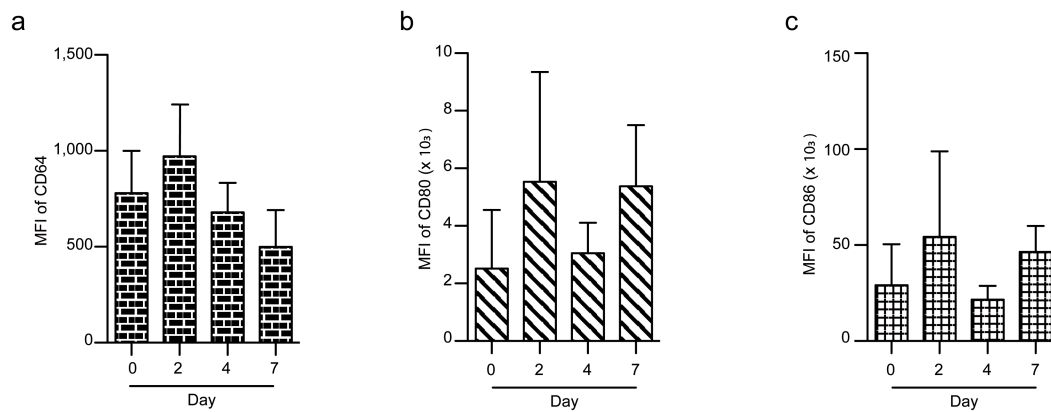
The protein band intensity was quantified with the Image J software 1,47V and normalized to the actin band. Ratios (protein / actin) were then compared between the different conditions. Fold changes of IRF5 and p21 expression were calculated by comparing the normalized value of IRF5 and p21 from the IFN- $\gamma$ -treated samples to the normalized value of IRF5 and p21 from the dM (US) control from the same donor.

### **HIV-1 DNA quantitative PCR (qPCR)**

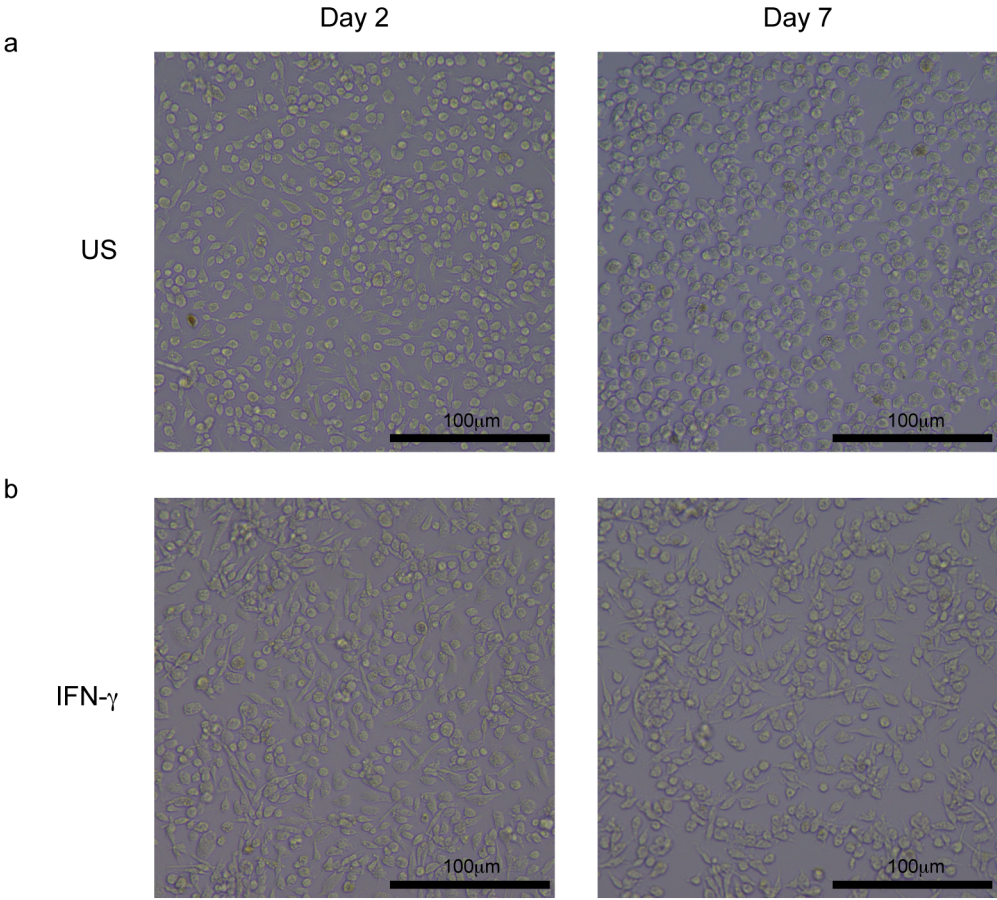
Total DNA in HIV-1/VSV-G-infected dM was extracted 72 h postinfection (p.i.) by using the DNeasy kit as recommended by the manufacturer (Qiagen, California, USA). Quantitative real-time PCR analysis of late (U5GAG) forms of viral DNA was carried on an ABI Prism 7500 sequence detection system as previously described<sup>19</sup>. Standards for U5GAG amplification products were generated by serial dilution of DNA extracted from HIV-1 8E5 cells containing one integrated copy of HIV-1 per cell. Integrated HIV-1 DNA was quantified by real-time Alu-LTR nested PCR using primers and probes described elsewhere, with some modifications<sup>19</sup>. Briefly, the first round of amplification was performed on a GeneAmp PCR system 9700 (Applied Biosystems, Saint Aubin, France). Integrated HIV-1 sequences were amplified by using the Expand High Fidelity kit (Roche, Meylan, France), two Alu primers (Alu F and Alu R)

and an LTR primer extended with an artificial tag sequence at the 5' end of the oligonucleotide (NY1R). Real-time nested PCR was run on the ABI Prism 7500 system using a 1/10 dilution of the first-round PCR product as template (primers NY2F and NY2R; probe NY2Alu). The integrated HIV-1 DNA copy number was determined with reference to a standard curve generated by concurrent amplification of HeLa R7 Neo cell DNA. A nested PCR conducted in parallel without the Alu primers in the first round gave a very weak background signal. The number of integrated HIV-1 DNA copies was obtained by subtracting the copy number measured without the Alu primers in the first round from the copy number measured in the full reaction. The amount of viral DNA was normalized to the endogenous reference albumin gene (for total DNA extracts). Standard curves were generated by serial dilution of a commercial human genomic DNA (Roche, Meylan, France).

### Supplementary Figure S1

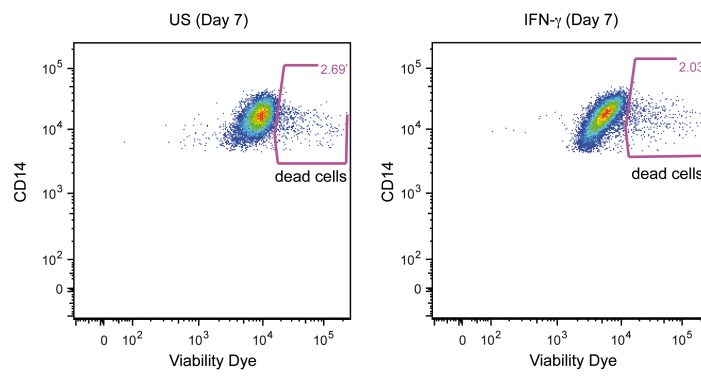


Supplementary Figure S2



## Supplementary Figure S3

a



b

